Soft Matter

Temperature Dependent Perylene Fluorescence as a Probe of Local Polymer Glass Transition Dynamics

Journal:	*Soft Matter*
Manuscript ID	SM-ART-04-2022-000552.R2
Article Type:	Paper
Date Submitted by the Author:	21-Jul-2022
Complete List of Authors:	Han, Yixuan; Emory University, Department of Physics Roth, Connie; Emory University, Department of Physics

Temperature Dependent Perylene Fluorescence as a Probe of Local Polymer Glass Transition Dynamics

Yixuan Han and Connie B. Roth*
Department of Physics, Emory University, Atlanta, Georgia 30322 USA

*Author to whom correspondence should be addressed: cbroth@emory.edu

Submitted to *Soft Matter*, April 29, 2022; revised version submitted June 20, 2022, 2nd revision submitted July 21, 2022

Abstract: We demonstrate how the temperature dependence of perylene's fluorescence emission spectrum doped in bulk polymer matrices is sensitive to the local glass transition dynamics of the surrounding polymer segments. Focusing on the first fluorescence peak, we show that the intensity ratio $I_{\rm Ratio}(T) = I_{\rm Peak}(T)/I_{\rm SRR}$ between the first peak and a self referencing region (SRR) has a temperature dependence resulting from the temperature-dependent nonradiative decay pathway of the excited perylene dye that is influenced by its intermolecular collisions with the surrounding polymers segments. For different polymer matrices, poly(methyl methacrylate) (PMMA), polystyrene (PS), poly(2-vinyl pyridine) (P2VP), and polycarbonate (PC), we demonstrate that $I_{\rm Ratio}(T)$ exhibits a transition from a non-Arrhenius behavior above the glass transition temperature $T_{\rm g}$ of the polymer to an Arrhenius temperature dependence with constant activation energy E below the $T_{\rm g}$ of the polymer matrix, indicating perylene's sensitivity to cooperative α-relaxation dynamics of the polymer matrix. This transition in temperature dependence allows us to identify a perylene defined local $T_{\rm g}{}^{\rm perylene}$ of the surrounding polymer matrix that agrees well with the known $T_{\rm g}$ values of the polymers. We define a fluorescence intensity shift factor $c_f \log\left(\frac{I_{\rm Ratio}(T)}{I_{\rm Ratio}(T_{\rm ref})}\right) \equiv \log(a_T)$ in analogy with the Williams-Landel-Ferry (WLF) equation and use literature WLF parameters for the polymer matrix to quantify the calibration factor c_f needed to convert the fluorescence intensity ratio to the effective time scale ratio described by the conventional WLF shift factor. This work opens up a new characterization method that could be used to map the local dynamical response of the glass transition in nanoscale polymer materials using appropriate covalent attachment of perylene to polymer chains.

1. Introduction

Nanostructured multi-component materials such as polymer nanocomposites and nanostructured polymer blends, as well as nanoconfined thin films have material properties dominated by interfaces. These interfaces cause perturbations to local material properties resulting in strong spatial gradients in dynamics and likely numerous other related properties.[1–4] A major open question in the field is the nature of these spatial gradients and how they are interrelated. To characterize these effects, new experimental methods are needed that can measure local material properties in order to construct a picture of how spatial variations in different interrelated properties change near interfaces. The first step to the development of such techniques is the characterization of the new method in bulk materials where the measured values can be compared to known bulk properties. To that end, we present here a characterization of the temperature dependence of perylene's fluorescence spectrum in bulk polymer matrices demonstrating its sensitivity to local polymer dynamics consistent with bulk α-relaxations above the glass transition temperature $T_{\rm g}$ and β-relaxations below $T_{\rm g}$. As a molecular dye, perylene's fluorescence spectrum is impacted by the local polymer environment around it, making perylene a probe of local polymer mobility that with appropriate chemical labeling could be used to interrogate local polymer dynamics within nanostructured materials.

Fluorescent probes have been frequently used to characterize material changes within the local environment of the probe based on a dye's intrinsic sensitivity to parameters such as temperature, viscosity, polarity, and pressure.[5] A well-known example is pyrene, which has been widely used as an indicator of local polarity in solutions via what is referred to as the Py-scale, characterizing the intensity ratio between the first and third vibronic bands of the fluorescence emission spectrum of pyrene.[5,6] In polymers, pyrene's sensitivity to local polarity, stiffness, and pressure has been used to measure the local glass transition temperature $T_{\rm g}$,[7–9] stiffness,[10,11] and phase separation.[12] Pyrene, like perylene, is part of a class of fluorescent probes that exhibit changes in their fluorescence emission spectrum resulting from perturbations in their vibronic band structure that reflect the probe's local environment. Other classes of fluorescent probes exploit the rotational or translational motion of the dye to interpret local mobility of polymer matrices. For example, rotor dyes have been used to monitor physical aging.[13–15] In addition, the reorientation of fluorescent probes has been used to monitor the segmental dynamics of the near free surface region in polymer thin films[16–18] and near polymer interfaces.[19,20] Translational diffusion parallel[21–23] and perpendicular[24] to the substrate have also been studied in polymer thin films.

Perylene, as a polycyclic aromatic hydrocarbon fluorophore, has been reported as having good thermal stability at high temperature and a high quantum yield in its fluorescence emission,[25] making it an ideal choice as a molecular probe for polymer thin films. Perylene incorporated in polymer binders has been used as temperature-sensitive paints (TSP) for real-time monitoring of the surface temperature distribution in the aerodynamics community.[26,27] A dual-component molecular thermometer consisting of perylene and another non-emissive molecule was reported to show ratiometric variation upon changes in temperature, due to the change in the shape of the emission spectrum via the exciplex formation between the two components.[28] Bur et al. have measured emission spectra at different temperatures for perylene doped in polycarbonate (PC), where they found that the intensity ratio of the second peak to the first trough shows a linear dependence on temperature.[25] Due to this linear temperature dependence, perylene has been used as a molecular thermometer, as reported in a later study where perylene was doped in poly(acrylonitrile) (PAN) to monitor temperature perturbations caused by embedded metal nanoparticles.[29] Nevertheless, the mechanism of the temperature dependence of perylene and how the temperature dependence of perylene is influenced by the surrounding polymer matrix is little studied.

Temperature is an important intensive parameter that strongly impacts the dynamics of polymers, as well as the emission of fluorophores embedded in the polymer matrices. When the electrons of a fluorophore in the higher energy excited states return to the ground state, the excess energy will be dissipated either through a radiative transition (observed as fluorescence) or a nonradiative transition (e.g., vibrational relaxation and collision with surrounding molecules).[5] The rate of nonradiative decay increases with increasing temperature as the local mobility of the surrounding polymer's segmental dynamics increases, leading to a suppression of fluorescence emission and a decrease in the emission intensity. Therefore, monitoring the emission intensity as a function of temperature can provide an indirect probe of the nonradiative decay rate that can then be correlated with the dynamics of the surrounding polymer matrix.

In the present work, we investigate the temperature dependence of perylene doped in various polymer matrices and assess the impact the surrounding polymer dynamics has on the fluorescence emission spectrum. We find a temperature-invariant region in the emission spectra collected at different temperatures, which we name as the self-referencing region (SRR). Normalizing to this self-referencing region provides an internal correction to account for fluctuations in the excitation intensity when characterizing the temperature dependence of the emission spectrum. The temperature dependence of the intensity ratio between the first peak I_{Peak} and this SRR I_{SRR} is reproducible for a given polymer. We find that the temperature dependence of this intensity ratio $I_{\mathrm{Ratio}}(T) = I_{\mathrm{Peak}}/I_{\mathrm{SRR}}$ reflects the temperature dependent dynamics of the surrounding polymer matrix. The measured intensity ratio corresponds to the quantum yield Φ of the fluorophore, reflecting the relative probability of the excited state perylene molecule decaying via the radiative pathway leading to fluoresced light versus some nonradiative decay pathway. The temperature dependence arises from the nonradiative decay mechanisms, where the probability of the excited state perylene molecule decaying via a nonradiative pathway varies with temperature depending on the dynamics of the surrounding polymer segments, i.e., altering the quantum yield for fluorescence. We define a fluorescence intensity "shift factor" a_T from the emission intensity ratio $I_{\mathrm{Ratio}}(T)$ with respect to that at a reference temperature T_{ref} taken to be the bulk glass transition temperature $T_{\mathrm{g}}^{\mathrm{bulk}}$ of the polymer matrix, in analogy to the shift factor a_T of the Williams-Landel-Ferry (WLF) equation. We find that the trend of this fluorescence defined $\log(a_T)$ vs $(1/T - 1/T_{\mathrm{ref}})$ shows a non-Arrhenius behavior in the supercooled liquid regime above $T_{\mathrm{g}}^{\mathrm{bulk}}$, suggesting that the nonradiative decay process is influenced by the cooperative α-relaxations of the surrounding polymer segments. In contrast, in the glassy regime below $T_{\mathrm{g}}^{\mathrm{bulk}}$ when cooperative motion arrests, the nonradiative decay follows a simple Arrhenius trend with a constant activation energy, consistent with the local β-relaxation.

2. Experimental Methods

Polystyrene (PS) with molecular weight $M_{\mathrm{w}} = 650$ kg/mol, $M_{\mathrm{w}}/M_{\mathrm{n}} = 1.06$ from Pressure Chemical, poly(methyl methacrylate) (PMMA) with $M_{\mathrm{w}} = 815$ kg/mol, $M_{\mathrm{w}}/M_{\mathrm{n}} = 1.09$, poly(2-vinyl pyridine) (P2VP) with $M_{\mathrm{w}} = 650$ kg/mol, $M_{\mathrm{w}}/M_{\mathrm{n}} = 1.08$ and polycarbonate (PC) with $M_{\mathrm{w}} = 28$ kg/mol, $M_{\mathrm{w}}/M_{\mathrm{n}} = 1.66$ from Scientific Polymer Products were used as received. Polymer solutions were prepared by dissolving PS or PMMA in toluene, P2VP in butanol, and PC in 1,1,2-trichloroethane. Perylene (Aldrich) was doped into polymer solutions at trace levels (0.15 wt%, corresponding to 0.06–0.14 mol%) to prevent aggregation and formation of excimer at high dye concentrations.[30] Experimentally we saw no evidence of excimer fluorescence indicating that the perylene dyes were isolated and well dispersed in the polymer matrices. The sample methodology we used follows that developed by the Torkelson group for pyrene, which demonstrated that pyrene doped at <0.2 mol% provides the same measure of T_{g} as labeling (chemically grafting) the dye to the polymer chain.[7,31]

Polymer films were made by spin-coating polymer solutions onto 25 mm × 25 mm × 3.7 mm fused silica (SCHOTT) for fluorescence measurements and 20 mm × 20 mm silicon wafers (Wafernet) for film thickness measurements. Film thicknesses of the polymer films were measured by spectroscopic ellipsometry (Woollam M-

2000). Raw $\Psi(\lambda)$ and $\Delta(\lambda)$ data for $\lambda = 400 - 1000$ nm were fit to an optical layer model to obtain the polymer film thickness h. The optical layer model consisted of a transparent Cauchy layer, $n(\lambda) = A + B/\lambda^2$ for the polymer film, and a 1.25-nm-thick native oxide layer atop a semi-infinite silicon substrate. Film thicknesses of the films spin-coated on to fused silica were assumed to be the same as that spin-coated on to silicon wafers at identical spin speeds and solution concentrations. Bulk T_g values were determined by ellipsometry measurements of the temperature dependent film thickness $h(T)$ on cooling at 1 K/min, where values of T_g^{bulk} were found to be 96 °C for PS, 115 °C for PMMA, 94 °C for P2VP, and 150 °C for PC.

Steady state fluorescence spectra were acquired by a Photon Technology International QuantaMaster spectrometer. Samples were covered by a clear quartz piece with the same dimension as the fused silica substrate to limit oxygen quenching and sublimation of the fluorophore. The doped perylene was excited at 390 nm for PMMA and 394 nm for PS, P2VP and PC via a xenon arc lamp with an excitation bandpass of 3 nm and an emission bandpass of 5 nm. All films were annealed on the fluorometer heater (Instec HCS402) at $T_g^{bulk} + 35$ K for 20 min to remove thermal history of the polymer matrix. Although this annealing protocol is limited to prevent sublimation of the perylene dye, this protocol has been shown to be sufficient to relax the polymer conformation locally and give reproducible measures of the glass transition consistent with longer annealing histories for polymer thin films.[31–33] Emission spectra were collected on cooling at different temperatures. Full emission spectra (425-525 nm) were collected at $T_g^{bulk} + 35$ K, $T_g^{bulk} - 5$ K and $T_g^{bulk} - 45$ K with respect to the T_g of each polymer. Shorter spectra focused on the first peak and the self-referencing region (SRR) were collected between $T_g^{bulk} + 35$ K and $T_g^{bulk} - 45$ K in increments of 2 K and 10 K. The span of this shorter spectrum was 15 nm where the specific wavelength range varied slightly depending on the polymer matrix. The system was always cooled at 2 K/min between temperature settings. At the end of a cooling run, all samples were reheated to the initial temperature to verify that the initial emission intensity was recovered and ensure no photobleaching had occurred during the course of the experiment.

3. Results and Discussion

We start by comparing the fluorescence emission spectrum of perylene doped into various polymer matrices in the glassy state at a consistent temperature that is 45 K below the bulk glass transition temperature T_g^{bulk}. **Figure 1** demonstrates the normalized emission intensity as a function of wavelength for four bulk polymer films of thickness h: PS ($h = 360$ nm), PMMA ($h = 282$ nm), P2VP ($h = 262$ nm), and PC ($h = 541$ nm). The emission spectra were normalized to the interval between zero and one, based on the intensity of the first peak, for comparison. Across the different polymer matrices, the emission spectra of perylene are in general similar, with small variations in the peak locations and relative intensities of the peaks. PS and PC show similar spectral structure with the first, second, and third peaks located at approximately 445, 475, and 507 nm, respectively. In contrast, the spectrum of PMMA exhibits a blue shift of ≈4 nm with respect to PS and PC, while the spectrum of P2VP exhibits a red shift of ≈2 nm. Such blue and red shifts result from differences in polarity of the polymer matrices. With the intensity of the first peak normalized to one, we can also observe small variations in the relative intensities of the rest of the peaks. In PMMA and PS matrices, perylene shows similar magnitudes of the second and third peaks, relative to the first peak, which are both slightly lower than the strength of the second and third peaks in the P2VP and PC matrices. The difference in the relative strength of the peaks suggest small changes are occurring in the vibronic bands of perylene, reflecting perturbations to its intramolecular vibrations caused by the surrounding polymer.

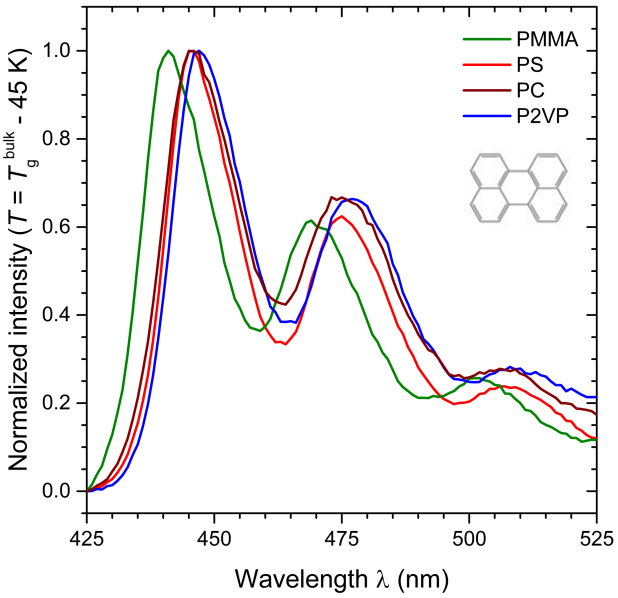

Figure 1: Normalized fluorescence emission intensity as a function of wavelength for perylene doped (0.15 wt%) in bulk polymer films: PS (red), PMMA (green), P2VP (blue), and PC (brown), all in the glassy state at $T = T_g^{bulk} - 45$ K. The perylene probe is excited at 390 nm for PMMA and 394 nm for PS, P2VP and PC. Emission intensities are normalized to between [0,1]. Inset shows the chemical structure of perylene.

To investigate the temperature dependence of perylene doped in polymer matrices, emission spectra were collected at three different temperatures in distinct regimes with respect to T_g^{bulk}: high temperature at $T_g^{bulk} + 35$ K deep in the equilibrium liquid regime, medium temper-

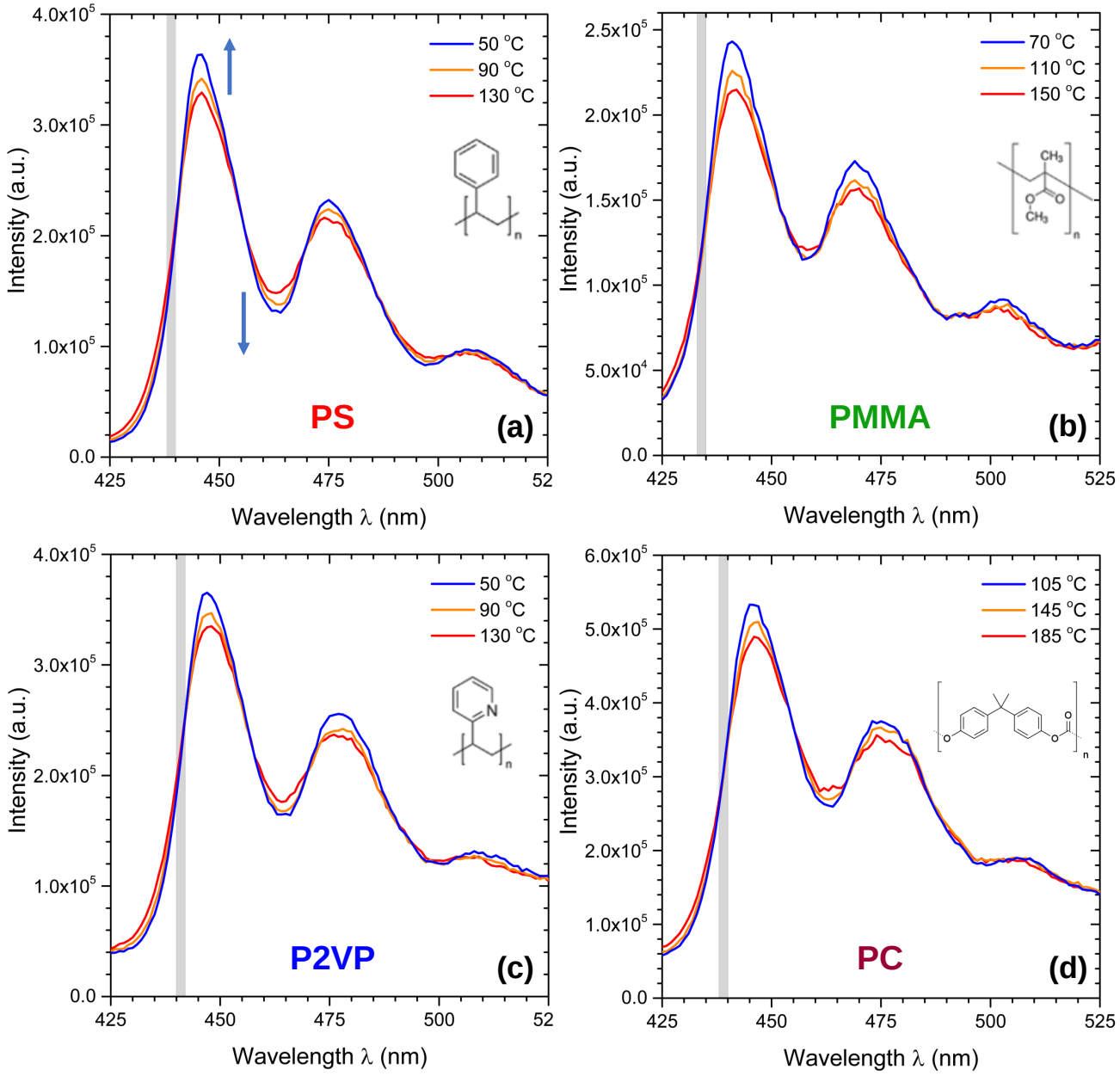

Figure 2: Fluorescence emission intensity as a function of wavelength at different temperatures (red curves are at a high temperature of T_g^{bulk} + 35 K, orange curves are at a medium temperature of T_g^{bulk} − 5 K, and blue curves are at a low temperature of T_g^{bulk} − 45 K) for perylene doped in bulk polymer films: (a) PS, (b) PMMA, (c) P2VP, and (d) PC. Self-referencing region (SRR) is represented by the light gray bar, indicating the part of the spectrum that is invariant at different temperatures. Blue arrows represent the shifts in the spectra with decreasing temperature. Inset shows the corresponding chemical structure of the polymers.

ature at T_g^{bulk} − 5 K near the glass transition, and low temperature at T_g^{bulk} − 45 K deep in the glassy regime. **Figure 2** shows the emission intensity as a function of wavelength for perylene doped in bulk polymer films (same samples as in Fig. 1) at different temperatures. The observed shifts to the spectra of perylene with temperature are similar for all four polymer matrices, where the magnitudes of the first and second peak increase with decreasing temperature and the magnitude of the first trough decreases with decreasing temperature. The increase in overall emission intensity with decreasing temperature can be explained by the decrease in the probability of nonradiative decay at lower temperatures.

One interesting feature of the temperature dependent spectra is that the spectrum does not increase uniformly at all wavelengths as the temperature decreases. Instead,

some locations of the spectrum move in the opposite direction to that of the peaks, resulting in regions where the intensity is invariant as temperature changes. Such regions are often referred to as isosbestic points.[34] We chose to name the temperature invariant region to the left of the first peak as the self-referencing region (SRR), and use it to account for any fluctuations to the overall magnitude of the spectrum which can be subject to perturbations (e.g. fluctuations in excitation light intensity) not reflective of changes in temperature. Therefore, the intensity ratio between the intensity of the first peak I_{Peak} and the intensity of the SRR I_{SRR},

$$I_{\mathrm{ratio}} = \frac{I_{\mathrm{Peak}}}{I_{\mathrm{SRR}}} , \qquad (1)$$

should not be influenced by the fluctuations in excitation light intensity, compared with solely measuring the peak intensity I_{Peak}. In practice, we find that for bulk films with different film thicknesses, the SRR for a given polymer consistently falls within a span of 2 nm on the wavelength axis, which we defined as the width of the SRR, confirming that the existence of the SRR is a characteristic feature of perylene doped in the polymer matrices. The locations of the SRR are represented by gray bars in Fig. 2. In contrast to the uniform width of the SRR, the location of the SRR depends on the specific polymer matrix that perylene is doped into. Specifically, the SRR is located at 438-400 nm for PS and PC, at 433-435 nm for PMMA and 440-442 nm for P2VP. The relative locations of the SRRs for the different polymers agree with the blue and red shifts of the emission spectrum shown in Fig. 1, suggesting that the SRR is a fundamental feature of the perylene emission spectrum while the location of the SRR is altered by the polarity of the surrounding polymer matrices that shift the emission spectrum.

We now examine more closely how the spectrum of perylene doped in polymer matrices changes relative to the SRR at various temperatures. To minimize the amount of exposure to the excitation light the sample experiences and reduce photobleaching, a short wavelength range (span = 15 nm) that includes the SRR and the first peak is selected instead of the full spectrum scan (span = 100 nm). The exact wavelength range of the short emission scan varies with the specific positions of the first peak and the SRR in the polymer matrix, with a fixed span of 15 nm. With this reduced range of emission scan, the temperature dependence can be characterized at a finer resolution (e.g. every 10 K) than the high, medium, and low temperature settings shown in Fig. 2. These short wavelength range emission spectra were acquired every 10 K during cooling from $T_{\mathrm{g}}^{\mathrm{bulk}}$ + 35 K to $T_{\mathrm{g}}^{\mathrm{bulk}}$ − 45 K at a cooling rate of 2 K/min. No noticeable photobleaching was observed after reheating to the initial temperature for samples measured following this procedure. **Figure 3** demonstrates the emission spectra (spanning a wavelength range from 431-446 nm) of a 444-nm-thick PMMA film measured at different temperatures upon cooling. The emission spectra collected from high temperature ($T_{\mathrm{g}}^{\mathrm{bulk}}$ + 35 K) to low temperature ($T_{\mathrm{g}}^{\mathrm{bulk}}$ − 45 K) are graphed in varying colors from red to green, with the SRR at 434 nm and the peak at 441 nm marked. With decreasing temperature, the intensity at the SRR I_{SRR} remains invariant, while the intensity at the peak I_{Peak} increases monotonically. We are interested in the temperature dependence of the peak to SRR intensity ratio for different polymers. This intensity ratio $I_{\mathrm{Peak}}/I_{\mathrm{SRR}}$ likely reflects information about the physical and dynamical properties of the polymer matrices around the perylene dye. Previous ratiometric measurements have reported that the intensity ratio between the second peak and the first trough of the perylene spectrum changes linearly with temperature.[25,29] Due to our selection of the first peak and the SRR, the temperature dependence of the intensity ratio $I_{\mathrm{Peak}}/I_{\mathrm{SRR}}$ is possibly different than that reported in the literature for the alternate ratio, perhaps revealing different local properties than simply a temperature dependence.

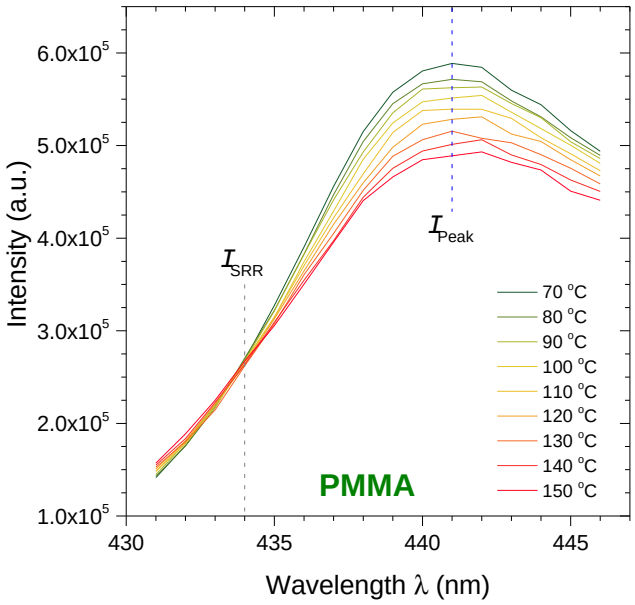

Figure 3: Fluorescence emission spectra at different temperatures focused on the first peak for perylene doped in a bulk PMMA film (h = 444 nm). The emission spectra were collected at every 10 K from $T_{\mathrm{g}}^{\mathrm{bulk}}$ + 35 K to $T_{\mathrm{g}}^{\mathrm{bulk}}$ − 45 K on cooling at 2 K/min. The locations of the SRR and the first peak are 434 nm and 441 nm, respectively.

To further characterize the temperature dependence of the $I_{\mathrm{Peak}}/I_{\mathrm{SRR}}$ intensity ratio, we reduce the step size of the temperature ramp from 10 K to 2 K to increase the number of data points. Following this procedure, scans of the short emission spectrum (span = 15 nm) that includes the first peak and the SRR were measured every 2 K on cooling from $T_{\mathrm{g}}^{\mathrm{bulk}}$ + 35 K to $T_{\mathrm{g}}^{\mathrm{bulk}}$ − 45 K with 2 K/min cooling rate between temperature steps. The intensity ratio I_{Ratio} (eq. 1) is calculated

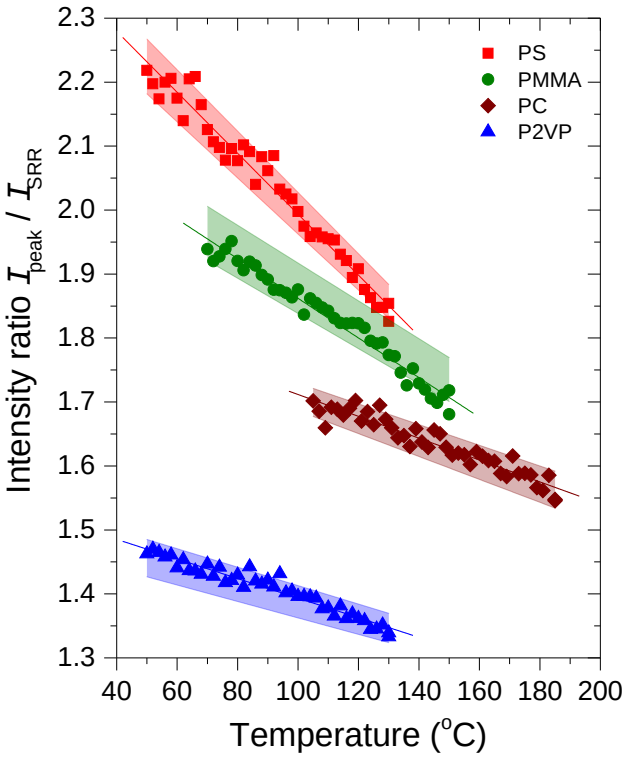

Figure 4: Temperature dependence of the intensity ratio $I_{\mathrm{Ratio}} = I_{\mathrm{Peak}}/I_{\mathrm{SRR}}$ for perylene doped in bulk films of different polymers: PS (red), PMMA (green), PC (brown), and P2VP (blue). Representative data sets are shown as solid symbols with corresponding linear fits. Shaded areas demonstrate the range of sample-to-sample variability between nominally identical samples.

as the peak intensity (averaged over a ±1 nm range) divided by the intensity of the SRR. **Figure 4** graphs the intensity ratio I_{Ratio} as a function of temperature for perylene doped in bulk films of the different polymers. A single representative data set for each polymer is shown as solid symbols while the shaded area demonstrates the sample-to-sample variability across nominally identical samples. For all four polymer matrices, the intensity ratio of the perylene probe shows a similar trend with temperature, where I_{Ratio} increases with decreasing temperature monotonically. These intensity ratio trends are reproducible for bulk films of the same polymer, where the reference to I_{SRR} can account for any fluctuations in the emission intensity of I_{Peak}. Such good reproducibility of I_{Ratio} suggests that the temperature dependence of the perylene probe reflects perturbations caused by the surrounding polymer matrix. To quantify the differences in the temperature dependent trends between polymers, we apply a simple linear fit to the data as a first order approximation. We find that the magnitudes of the slopes and intercepts of the linear fits vary depending on the polymer matrix. The values of the slopes of the linear trends are −0.00477 for PS, −0.00310 for PMMA, −0.00171 for PC, and −0.00153 for P2VP. The slopes of the temperature dependence between different polymers are similar for P2VP and PC, while the slope of PMMA is roughly twice of that for P2VP and the slope of PS is roughly three times of that for P2VP. To compare the intercepts of the linear fits without extrapolation, we compare the magnitude of I_{Ratio} at the same temperature ($T = 120$ °C) for different polymers. The values of $I_{\mathrm{Ratio}}(T = 120\ ^{\circ}\mathrm{C})$ are 1.895 for PS, 1.797 for PMMA, 1.680 for PC, and 1.366 for P2VP. It is interesting that polymers with larger slopes tend to also have a larger magnitude of I_{Ratio} at a given temperature.

To understand the mechanism behind the different temperature dependencies of the intensity ratio I_{Ratio} of perylene in different polymers, we need to explore how the probability of fluorescence emission of a photon is impacted by temperature. Fundamentally, the decrease in the fluorescence emission intensity at higher temperature results from a larger probability of energy decay from the excited electronic state by nonradiative pathways via intramolecular vibrations of the perylene dye and intermolecular collisions of the dye with the surrounding polymer matrix. Therefore, the temperature dependence of the emission intensity ratio I_{Ratio} can be described by the temperature dependence of the rate of nonradiative decay. Such rate parameters represent the probability of a certain electronic transition occurring under a given condition. The efficiency of the fluorophore to radiate energy is characterized by its quantum yield Φ, defined as the ratio of the emission light intensity I_{F} to the excitation light intensity I_{E}: $\Phi = \frac{I_{\mathrm{F}}}{I_{\mathrm{E}}}$.[5] The quantum yield Φ can also be written as the ratio of the rate parameters $\Phi = \frac{k_{\mathrm{R}}}{k_{\mathrm{R}}+k_{\mathrm{NR}}}$, where k_{R} is the rate of radiative decay (fluorescence emission) and k_{NR} is the rate of nonradiative decay.[5]

Previous studies have demonstrated that the temperature dependence of the nonradiative decay rate k_{NR} can be treated as a sum of a temperature invariant part k_0 and a temperature dependent part k_1, where k_1 has been shown experimentally to follow an Arrhenius temperature dependence,[26,35,36]

$$k_{\mathrm{NR}} = k_0 + k_1 = k_0 + A\exp\left(-\frac{E}{k_{\mathrm{B}}T}\right), \qquad (2)$$

when the dyes have been in liquids or polymers well in their glassy state. E is the activation energy associated with the nonradiative decay, A is a prefactor, k_{B} is Boltzmann's constant, and T is the absolute temperature. By incorporating such a temperature dependence for the nonradiative decay rate k_{NR}, the ratio of $\frac{I_{\mathrm{E}}}{I_{\mathrm{F}}(T)} = \Phi^{-1} = \frac{k_{\mathrm{R}}+k_{\mathrm{NR}}}{k_{\mathrm{R}}}$ can be written as

$$\frac{I_{\mathrm{E}}}{I_{\mathrm{F}}(T)} = \frac{k_{\mathrm{R}} + \left[k_0 + A\exp\left(-\frac{E}{k_{\mathrm{B}}T}\right)\right]}{k_{\mathrm{R}}}\ . \qquad (3)$$

The temperature invariant parts can be canceled by considering the difference of this ratio at the desired temperature T to that at absolute zero $T = 0$, resulting in

a purely temperature dependent term $\Omega(T)$:[26,27]

$$\Omega(T) = \frac{I_E}{I_F(T)} - \frac{I_E}{I_F(0)} = \frac{A}{k_R} \exp\left(-\frac{E}{k_B T}\right) . \quad (4)$$

This assumes that the radiative decay rate k_R is independent of temperature, which is reasonable for an electronic energy level transition. We next consider a ratio of the quantity $\Omega(T)$ at the desired temperature T relative to a reference temperature T_{ref}:

$$\frac{\Omega(T_{ref})}{\Omega(T)} = \exp\left[\frac{E}{k_B}\left(\frac{1}{T} - \frac{1}{T_{ref}}\right)\right] , \quad (5)$$

which based on the first half of eq. 4 can also be written as

$$\frac{\Omega(T_{ref})}{\Omega(T)} = \left[\frac{I_F(0) - I_F(T_{ref})}{I_F(0) - I_F(T)}\right] \frac{I(T)}{I(T_{ref})} . \quad (6)$$

When T does not deviate too far from the reference temperature T_{ref} on an absolute temperature scale, the term in square brackets is ≈1 leaving[26,27]

$$\frac{I(T)}{I(T_{ref})} = \exp\left[\frac{E}{k_B}\left(\frac{1}{T} - \frac{1}{T_{ref}}\right)\right] \quad (7)$$

when combined with eq. 5. Therefore, the fluorescence intensity at a given temperature T relative to that at a reference temperature T_{ref} can be written in an Arrhenius form:[5,26,27]

$$\log\left[\frac{I(T)}{I(T_{ref})}\right] = \frac{E}{k_B}\left(\frac{1}{T} - \frac{1}{T_{ref}}\right) . \quad (8)$$

Following this reasoning, we graph the temperature dependence of $I_{Ratio}(T)$ in this form following eq. 8, noting that $\frac{I_{Ratio}(T)}{I_{Ratio}(T_{ref})} = \frac{I_{Peak}(T)}{I_{Peak}(T_{ref})}$ as I_{SRR} is independent of temperature. **Figure 5** illustrates the observed behavior of perylene doped in bulk PMMA films with $\log\left[\frac{I_{Ratio}(T)}{I_{Ratio}(T_{ref})}\right]$ graphed as a function of $\left(\frac{1}{T} - \frac{1}{T_{ref}}\right)$, where we have chosen T_g^{bulk} as the reference temperature T_{ref}. A representative data set from a single sample is shown as green circles, while additional data denoted as gray circles demonstrate the sample-to-sample variability of nominally identical samples. Graphed in this manner, we find that the temperature dependence of $I_{Ratio}(T)$ follows a linear Arrhenius trend with constant activation energy E for temperatures below T_g^{bulk}. At T_g^{bulk}, we observe a distinctive change in the slope of the Arrhenius plot, where over multiple data sets we have come to conclude that the $I_{Ratio}(T)$ data follow a non-Arrhenius temperature dependence with a temperature dependent activation energy $E(T)$ for temperatures above T_g^{bulk}. This transition point at T_g^{bulk} is independent of the choice of T_{ref}, where we have tested various choices of T_{ref} and found no changes to the transition point that always occurs at the T_g of the polymer matrix. This also indicates that the temperature dependence of $I_{Ratio}(T)$ as plotted in Fig. 4 is not strictly linear, but simply that the transition that occurs at T_g^{bulk} is not distinctive enough when plotted in this way. A strictly linear trend in $I_{Ratio}(T)$ does not exhibit the same behavior as shown in Fig. 5.

The observation of a non-Arrhenius temperature dependence above the glass transition temperature of the polymer matrix is not surprising as the nonradiative decay pathways are sensitive to the local dynamics of the polymer segments surrounding the dye.[5] At higher temperatures when the local dynamics of the polymer are more active, there will be a higher probability for the excited state dye to decay to its ground state via some nonradiative decay pathway than the radiative decay pathway that we measure experimentally as fluoresced light. The temperature dependence of the fluorescence intensity represents this change in the relative probability of decay pathways for the excited state dye and will therefore reflect the dynamics of the surrounding polymer.

The activation energy $E(T)$ corresponds to energy loss

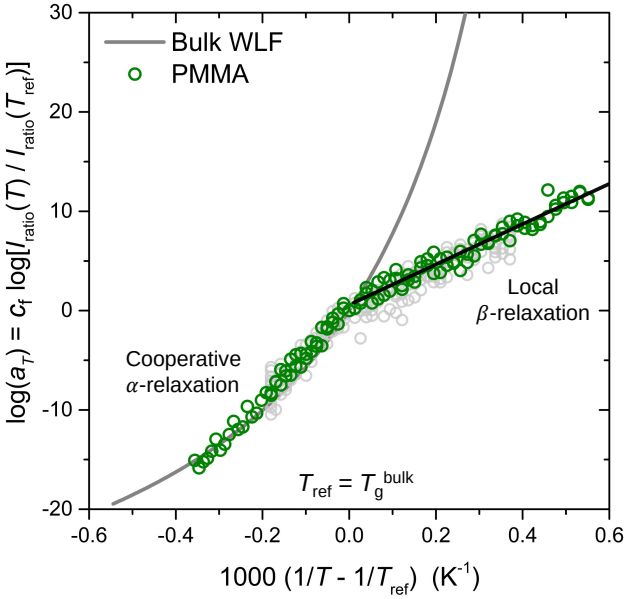

Figure 5: Temperature dependence of the fluorescence intensity shift factor $\log(a_T) = c_f \log[I_{Ratio}(T)/I_{Ratio}(T_{ref})]$ for perylene doped in bulk PMMA films. A single representative data set is shown as green circles, while gray circles represent additional samples demonstrating sample-to-sample reproducibility across nominally identical samples. Graphed on this Arrhenius plot, the slope of the data show a distinctive change at the polymer matrix's glass transition temperature T_g^{bulk} (taken as T_{ref}). Bulk WLF parameters from the literature[37] (gray curve) were used to determine the calibration factor c_f that defines the vertical scale from the fluorescence intensity. A linear fit is applied to the data below T_g^{bulk} (black line) to determine the activation energy E in the glassy regime.

of the excited state perylene dye via nonradiative decay mechanisms that are reflective of the local dynamics of the surrounding polymer matrix. Thus, the observed transition from a non-Arrhenius to an Arrhenius temperature dependence as the polymer matrix transitions from the supercooled liquid regime above T_g to the glassy regime below T_g reflects the change in temperature-dependent polymer dynamics of the matrix surrounding the dyes. We can use literature values for the non-Arrhenius temperature dependence to quantify the scale of the $\log\left[\frac{I_{\text{Ratio}}(T)}{I_{\text{Ratio}}(T_{\text{ref}})}\right]$ axis by making an analogy with the Williams-Landel-Ferry (WLF) equation. The WLF equation,

$$\log(a_T) = -\frac{C_1\,(T - T_{\text{ref}})}{C_2 + (T - T_{\text{ref}})}\ , \tag{9}$$

is commonly used to describe the non-Arrhenius temperature dependence of polymer materials in their rubbery, supercooled liquid regime above T_g, where values of the constants C_1 and C_2 are tabulated for various polymers with the reference temperature T_{ref} usually taken as T_g.[37–39] It is mathematically equivalent to the Vogel-Fulcher-Tammann (VFT) equation commonly used to describe the supercooled liquid regime of various glass formers.[40]

Similar to how the WLF equation is routinely defined based on a viscosity $\log\left[\frac{\eta(T)}{\eta(T_{\text{ref}})}\right]$ or relaxation time $\log\left[\frac{\tau(T)}{\tau(T_{\text{ref}})}\right]$ ratio, we use the fluorescence intensity ratio to define an equivalent a_T shift factor as:

$$c_f \log\left[\frac{I_{\text{Ratio}}(T)}{I_{\text{Ratio}}(T_{\text{ref}})}\right] \equiv \log(a_T) = \frac{E(T)}{k_B}\left(\frac{1}{T} - \frac{1}{T_{\text{ref}}}\right), \tag{10}$$

where we introduce a calibration factor c_f to connect the fluorescence intensity ratio to the effective time scale ratio described by the conventional WLF shift factor a_T. This calibration factor c_f depends on the specific polymer matrix, where tabulated literature values for the WLF parameters C_1 and C_2 are used to determine $\log(a_T)$ in eq. 9 and therefore c_f in eq. 10. Specifically this is done by graphing $\log\left[\frac{I_{\text{Ratio}}(T)}{I_{\text{Ratio}}(T_{\text{ref}})}\right]$ versus $-\frac{C_1\,(T-T_{\text{ref}})}{C_2+(T-T_{\text{ref}})}$ for $T \geq T_g^{\text{bulk}}$ and determining c_f from a one-parameter fit for the slope. For PMMA, the bulk WLF parameters were taken from Ref. 37 as $C_1 = 34$ and $C_2 = 80$ K at $T_{\text{ref}} = 393$ K, giving a calibration factor $c_f = 120$. This calibration factor acts to convert the vertical scale of the graph in Fig. 5 from the fluorescence intensity counts, which are in arbitrary units, to a meaningful scale that can then be compared with other experiments.

With this calibration of the fluorescence intensity ratio axis, we can then determine the effective activation energy E for the nonradiative decay of perylene in the polymer's glassy regime from the linear slope for temperatures $T < T_g^{\text{bulk}}$, which for PMMA is $E = 169 \pm 5$ kJ/mol. The dominant relaxation process below T_g upon cooling slowly through the glass transition as is done in the present experiments is the β-relaxation, along with other local segmental relaxations.[41,42] As such, we would expect these to be the primary local relaxations of the polymer segments surrounding the perylene dye contributing to its nonradiative decay in the polymer's glassy regime. Thus, it seems reasonable that the activation energy for the nonradiative decay of perylene is slightly larger but comparable to the activation energy for the β-relaxation of PMMA measured by dielectric spectroscopy, ~ 85 kJ/mol.[42] One might anticipate that a larger number of surrounding polymer segments and their local dynamics contribute to the nonradiative decay of perylene than that needed for a single β-relaxation event.

We next investigate how this measure of local polymer dynamics by perylene, reflected in the temperature dependence of the nonradiative decay rate, compares across different polymer matrices. **Figure 6** plots the fluorescence intensity shift factor $c_f \log\left[\frac{I_{\text{Ratio}}(T)}{I_{\text{Ratio}}(T_{\text{ref}})}\right] \equiv \log(a_T)$ as a function of $\left(\frac{1}{T} - \frac{1}{T_{\text{ref}}}\right)$ following eq. 10 for perylene doped in the different polymer matrices. We find that the temperature dependent trend of the fluorescence intensity ratio $I_{\text{Ratio}}(T)$ is similar for all polymers, following a non-Arrhenius temperature dependence above the polymer matrix's glass transition temperature and then transitioning to a linear Arrhenius trend below T_g^{bulk}. This is particularly distinctive for the $I_{\text{Ratio}}(T)$ data in the PS matrix shown in Fig. 6a where we have been able to extend the temperature range to higher temperatures. As we did for PMMA, tabulated literature values for the bulk WLF parameters of each polymer were used to define the fluorescence calibration factor c_f in eq. 10. The WLF parameters used were $C_1 = 12$ and $C_2 = 49$ K at $T_{\text{ref}} = 375$ K for PS giving a calibration factor $c_f(\text{PS}) = 45$, and $C_1 = 10.4$ and $C_2 = 52.2$ K at $T_{\text{ref}} = 426$ K for PC giving $c_f(\text{PC}) = 80$.[37] WLF parameters for P2VP were not found in the literature; thus, we chose to apply the WLF parameters of PS to P2VP given their similar T_g and chemical structure resulting in a calibration factor of $c_f(\text{P2VP}) = 100$ for P2VP. Using these calibration factors, as was done for PMMA above, we can determine an effective activation energy E for the nonradiative decay of perylene within a given polymer matrix based on the linear slope of the data in the glassy regime resulting in $E = 79 \pm 5$ kJ/mol for PS, $E = 81 \pm 9$ kJ/mol for P2VP, and $E = 117 \pm 12$ kJ/mol for PC. Unsurprising, the value of E for perylene in PS and P2VP are similar, likely reflecting comparable local dynamical environments.

The similarity between the temperature trends of perylene doped in the various polymer matrices confirms that the nonradiative decay process of perylene reflects changes in the local polymer dynamics. For an electron in the excited state of perylene, it will return to the

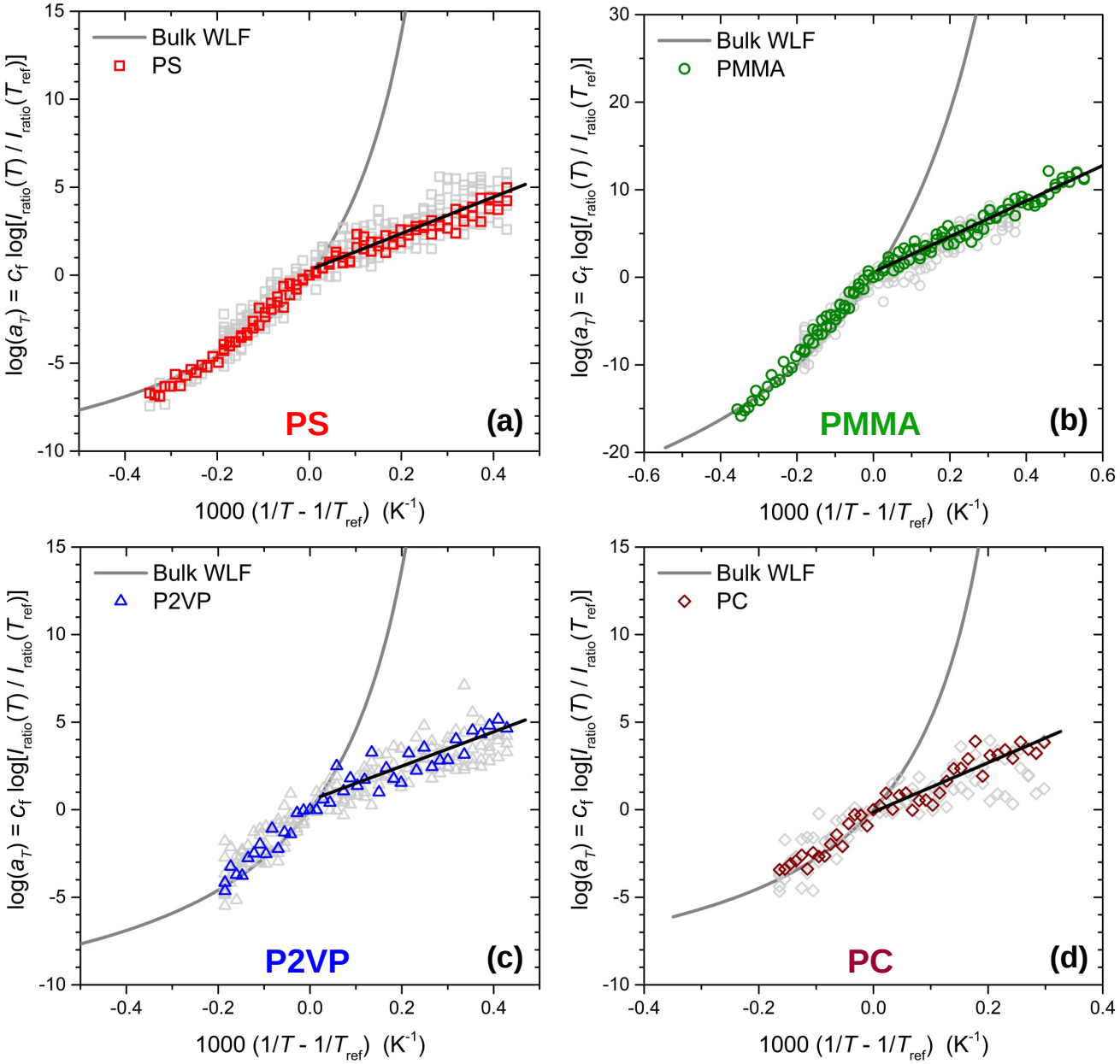

Figure 6: Temperature dependence of the fluorescence intensity shift factor $\log(a_T) = c_f \log[I_{\mathrm{Ratio}}(T)/I_{\mathrm{Ratio}}(T_{\mathrm{ref}})]$ for perylene doped in bulk films of (a) PS, (b) PMMA, (c) P2VP, and (d) PC. Representative data sets are shown as colored symbols (PS: red squares, PMMA: green circles, P2VP: blue triangles, and PC: brown diamonds) with gray symbols corresponding to additional samples demonstrating sample-to-sample variability across nominally identical samples. Data for temperatures $T > T_{\mathrm{g}}^{\mathrm{bulk}}$ ($=T_{\mathrm{ref}}$) show a non-Arrhenius temperature dependence that transitions to an Arrhenius trend below $T_{\mathrm{g}}^{\mathrm{bulk}}$. Bulk WLF parameters from the literature[37] (gray curves) were used to determine the calibration factors c_f for perylene in each polymer matrix to define the vertical scale from the fluorescence intensity. Simple linear fits (black lines) are applied to the data below $T_{\mathrm{g}}^{\mathrm{bulk}}$ to determine the activation energy E in the glassy regime.

ground state via either the radiative transition or a nonradiative transition. The radiative transition leads to fluorescence where the population of the electrons going through this pathway are characterized by the emission intensity. In contrast, the rate of nonradiative transition can be inferred from the emission intensity since an increase in the nonradiative decay rate would suppress the emission intensity. Due to perylene's intermolecular collisions with the surrounding polymer segments, more energy is dissipated when the polymer segments

have a higher mobility at elevated temperature above the glass transition temperature T_g. As can be seen in Fig. 6, the temperature dependence of the fluorescence intensity ratio $I_{Ratio}(T)$ exhibits a distinctive change in the slope of the data on the Arrhenius plot characterizing the change in activation energy $E(T)$ with temperature. Above T_g, a non-Arrhenius behavior with a temperature dependent activation energy $E(T)$ is observed, especially for the extended temperature range of the PS data in Fig. 6a, while below T_g, a simple Arrhenius trend with constant activation energy E is found. It appears that the nonradiative decay process impacting perylene in the polymer's supercooled liquid regime above T_g is reflecting the cooperative α-relaxation of the surrounding polymer segments that slow down as the glass transition is approached. For the temperature region below T_g in the polymer's glassy state, the cooperative α-relaxation is frozen out, leaving the nonradiative decay process of perylene primarily affected by the local β-relaxation of the surrounding polymer with a temperature independent activation energy, resulting in a simple Arrhenius trend. We identify the inflection point in the $c_f \log\left[\frac{I_{Ratio}(T)}{I_{Ratio}(T_{ref})}\right] \equiv \log(a_T)$ data based on the intersection of the linear fit below T_g with the WLF curve for each of the polymer matrices and use it to define a local T_g value, $T_g^{perylene}$, based on the temperature at which the surrounding polymer matrix around the perylene dye transitions from a non-Arrhenius to Arrhenius behavior: $T_g^{perylene} = 391$ K for PMMA, $T_g^{perylene} = 373$ K for PS, $T_g^{perylene} = 372$ K for P2VP, and $T_g^{perylene} = 425$ K for PC. For each of the four polymer matrices, this perylene based T_g value is found to agree well with known T_g^{bulk} values for these polymers to within the approximately ± 5 K that the $T_g^{perylene}$ values can be determined from these data.

It appears that the fluorescence sensitivity of perylene to the local polymer matrix is distinctly different from that of pyrene. Perylene identifies a $T_g^{perylene}$ of the local polymer matrix that is sensitive to the polymer's dynamics, a so-called dynamic T_g. This is in contrast to pyrene whose sensitivity to local T_g of the polymer matrix arises through its sensitivity to local polarity, stiffness, and pressure,[5,6] where pyrene's measure of T_g has been shown to agree well with ellipsometry.[7,43] Such measures of T_g through the material's thermal expansion are considered a thermodynamic T_g.[44] Interestingly, experimental measures of dynamic and thermodynamic T_g have been shown to display different trends in the film-average glass transition temperature $T_g(h)$ of confined polymer films with decreasing film thickness h even within the same system, where several different possible explanations have been proposed to explain these differences.[45] Studies based on molecular dynamics simulations have argued that the differences between dynamic and thermodynamic film-average $T_g(h)$ measures likely arise from how these different experimental measures weight the locally fast and slow regions of the dynamical gradient in the film-average measurement.[46,47] To verify this interpretation experimentally, local measurements of both the dynamic and thermodynamic $T_g(z)$ as a function of position z from a perturbing interface would need to be compared along with their measured averages. With appropriate chemical labeling, perylene has the potential to provide such a local measure of dynamic $T_g(z)$ to complement the existing local pyrene measurements of thermodynamic $T_g(z)$. This difference in fluorescence sensitivity between perylene and pyrene may stem from the large difference in the excited state lifetimes of the two dyes: $\tau_{ex} = 6$ ns for perylene versus $\tau_{ex} \approx 430$ ns for pyrene.[5] It is pyrene's unusually long excited state lifetime that gives it its unique sensitivity to local polarity as the surrounding dipoles are able to reorient relative to pyrene's long-lived excited state dipole that is formed on excitation.[5,6] Thus, given these differences between perylene and pyrene dyes, we believe that future studies of local $T_g^{perylene}$ and the temperature dependence of perylene's fluorescence response near polymer interfaces may prove fruitful in better understanding local changes in polymer dynamics in nanoconfined systems.

4. CONCLUSIONS

In this study, we have demonstrated how perylene's fluorescence emission spectrum can be used to probe local polymer dynamics when doped in bulk PS, PMMA, P2VP, and PC matrices. By characterizing the temperature dependence of perylene's emission spectrum, we identified a temperature invariant region to the left of the first peak, which we defined as a self-referencing region (SRR). This SRR can be used to correct for fluctuations in excitation intensity. Focusing on the intensity ratio $I_{Ratio} = I_{Peak}/I_{SRR}$ between the first peak and this SRR, we showed that the temperature dependence of this intensity ratio $I_{Ratio}(T)$ is reproducible across different samples depending on the surrounding polymer matrix.

The temperature dependence of this intensity ratio $I_{Ratio}(T)$ results from the temperature dependence of the nonradiative decay pathway of the excited perylene dye that is influenced by its intermolecular collisions with the surrounding polymer segments, and characterized by an effective activation energy $E(T)$. We observe that perylene's $I_{Ratio}(T)$ follows a non-Arrhenius temperature dependence for temperatures above the polymer's glass transition temperature T_g in its supercooled liquid regime that transitions to an Arrhenius temperature dependence for temperatures below the polymer's T_g in its glassy regime, suggesting that the nonradiative decay process is influenced by the cooperative α-relaxation of the local polymer segments. We are able to use the known WLF dependence for the polymer matrices for $T > T_g$ from the literature to calibrate the fluorescence intensity ratio. For temperatures below the polymer's T_g where the cooperative α-relaxations of the polymer ma-

trix are arrested, $I_{\mathrm{Ratio}}(T)$ exhibits to an Arrhenius temperature dependence with a constant activation energy E indicating that the nonradiative decay process of perylene is primarily influenced by the local β-relaxations below T_{g}.

We defined a fluorescence intensity "shift factor" $c_f \log\left[\frac{I_{\mathrm{Ratio}}(T)}{I_{\mathrm{Ratio}}(T_{\mathrm{ref}})}\right] \equiv \log(a_T)$ based on a ratio in fluorescence intensity $I_{\mathrm{Ratio}}(T)$ at the given temperature T relative to a reference temperature T_{ref} taken to be $T_{\mathrm{g}}^{\mathrm{bulk}}$ of the polymer matrix. Using tabulated bulk WLF parameters for the different polymers, we determined the fluorescence calibration factor c_f that converts the fluorescence intensity ratio to the effective time scale ratio described by the conventional WLF shift factor $\log(a_T)$, which allowed us to quantify the effective activation energy E for perylene's nonradiative decay rate in the glass regime below T_{g}. These fluorescence data of perylene's temperature dependent nonradiative decay rate that reflect the local dynamics of the surrounding polymer matrix were used to define a perylene glass transition temperature ${T_{\mathrm{g}}}^{\mathrm{perylene}}$ that we find agrees well with the known glass transition temperature T_{g} values for these polymers. Future efforts will apply these methods utilizing perylene as a local probe of polymer dynamics in thin films via covalent attachment to polymer chains.

Author contributions

Y. Han conducted the experiments, deciding on methodology and analysis, and contributed to writing of the original draft and reviewing. C. B. Roth provided supervision, funding, conceptualization and visualization of the manuscript, and contributed to editing and reviewing of the manuscript.

Acknowledgments

The authors gratefully acknowledge support from the National Science Foundation Polymers Program (DMR-1905782) and Emory University, as well as useful discussions with James Kindt.

Conflict of interest

The authors declare no competing financial interest.

REFERENCES

1 M. D. Ediger and J. A. Forrest, *Macromolecules*, 2014, **47**, 471–478.

2 C. B. Roth, *Chemical Society Reviews*, 2021, **50**, 8050–8066.

3 B. D. Vogt, *Journal of Polymer Science Part B: Polymer Physics*, 2018, **56**, 9–30.

4 Y. Han and C. B. Roth, *Journal of Chemical Physics*, 2021, **155**, 144901.

5 B. Valeur and M. N. Berberan-Santos, *Molecular Fluorescence: Principles and Applications*, John Wiley & Sons, 2012.

6 K. Kalyanasundaram and J. K. Thomas, *Journal of the American Chemical Society*, 1977, **99**, 2039–2044.

7 C. J. Ellison and J. M. Torkelson, *Nature Materials*, 2003, **2**, 695–700.

8 C. J. Ellison and J. M. Torkelson, *Journal of Polymer Science Part B: Polymer Physics*, 2002, **40**, 2745–2758.

9 P. M. Rauscher, J. E. Pye, R. R. Baglay and C. B. Roth, *Macromolecules*, 2013, **46**, 9806–9817.

10 S. Askar, C. M. Evans and J. M. Torkelson, *Polymer*, 2015, **76**, 113–122.

11 S. Askar and J. M. Torkelson, *Polymer*, 2016, **99**, 417–426.

12 A. Kriisa, S. S. Park and C. B. Roth, *Journal of Polymer Science Part B: Polymer Physics*, 2012, **50**, 250–256.

13 R. D. Priestley, C. J. Ellison, L. J. Broadbelt and J. M. Torkelson, *Science*, 2005, **309**, 456–459.

14 R. D. Priestley, L. J. Broadbelt and J. M. Torkelson, *Macromolecules*, 2005, **38**, 654–657.

15 C. J. Ellison, S. D. Kim, D. B. Hall and J. M. Torkelson, *European Physical Journal E*, 2002, **8**, 155–166.

16 K. Paeng, S. F. Swallen and M. D. Ediger, *Journal of the American Chemical Society*, 2011, **133**, 8444–8447.

17 K. Paeng and M. D. Ediger, *Macromolecules*, 2011, **44**, 7034–7042.

18 K. Paeng, R. Richert and M. D. Ediger, *Soft Matter*, 2012, **8**, 819–826.

19 J. Choi, S. Lee, J. Choe, Y. Chung, Y. E. Lee, J. Kim, M. Kim and K. Paeng, *ACS Macro Letters*, 2019, **8**, 1181–1186.

20 Y. Chung, J. Nam, D. Son, H. Lee, M. Kim and K. Paeng, *Macromolecules*, 2021, **54**, 4546–4556.

21 B. Frank, A. P. Gast, T. P. Russell, H. R. Brown and C. Hawker, *Macromolecules*, 1996, **29**, 6531–6534.

22 J. M. Katzenstein, D. W. Janes, H. E. Hocker, J. K. Chandler and C. J. Ellison, *Macromolecules*, 2012, **45**, 1544–1552.

23 R. Katsumata, A. R. Dulaney, C. B. Kim and C. J. Ellison, *Macromolecules*, 2018, **51**, 7509–7517.

24 D. B. Hall and J. M. Torkelson, *Macromolecules*, 1998, **31**, 8817–8825.

25 A. J. Bur, M. G. Vangel and S. Roth, *Applied Spectroscopy*, 2002, **56**, 174–181.

26 B. Campbell, T. Liu and J. Sullivan, in *25th Plasmadynamics and Lasers Conference proceedings*, American Institute of Aeronautics and Astronautics, 1994, ch. Temperature sensitive fluorescent paint systems, pp. 2483–2501.

27 T. Liu, B. T. Campbell, S. P. Burns and J. P. Sullivan, *Applied Mechanics Reviews*, 1997, **50**, 227–246.

28 N. Chandrasekharan and L. A. Kelly, *Journal of the American Chemical Society*, 2001, **123**, 9898–9899.

29 S. Maity, J. R. Bochinski and L. I. Clarke, *Advanced Functional Materials*, 2012, **22**, 5259–5270.

30 F. Ito, Y. Kogasaka and K. Yamamoto, *Journal of Physical Chemistry B*, 2013, **117**, 3675–3681.

31 C. J. Ellison, M. K. Mundra and J. M. Torkelson, *Macromolecules*, 2005, **38**, 1767 – 1778.

32 M. K. Mundra, C. J. Ellison, R. E. Behling and J. M. Torkelson, *Polymer*, 2006, **47**, 7747–7759.

33 M. K. Mundra, C. J. Ellison, P. Rittigstein and J. M. Torkelson, *European Physical Journal Special Topics*, 2007, **141**, 143.

34 P. L. Geissler, *Journal of the American Chemical Society*, 2005, **127**, 14930–14935.

35 R. G. Bennett and P. J. McCartin, *Journal of Chemical Physics*, 1966, **44**, 1969–1972.

36 L. Song and M. Fayer, *Journal of Luminescence*, 1991, **50**, 75–81.

37 K. L. Ngai and D. J. Plazek, in *Physical Properties of Polymers Handbook*, ed. J. E. Mark, Springer, New York, 2nd edn., 2007, ch. 26, pp. 455–478.

38 J. D. Ferry, *Viscoelastic Properties of Polymers*, John Wiley & Sons, New York, 3rd edn., 1980.

39 M. L. Williams, R. F. Landel and J. D. Ferry, *Journal of the American Chemical Society*, 1955, **77**, 3701–3707.

40 C. B. Roth and R. R. Baglay, in *Polymer Glasses*, ed. C. B. Roth, CRC Press, 2016, ch. 1: Fundamentals of Polymers and Glasses, pp. 3–22.

41 R. Greiner and F. R. Schwarzl, *Rheologica Acta*, 1984, **23**, 378–395.

42 N. G. McCrum, B. E. Read and G. Williams, *Anelastic and Dielectric Effects in Polymer Solids*, John Wiley & Sons, New York, 1967.

43 S. Kim, S. A. Hewlett, C. B. Roth and J. M. Torkelson, *European Physical Journal E*, 2009, **30**, 83.

44 M. Alcoutlabi and G. B. McKenna, *Journal of Physics: Condensed Matter*, 2005, **17**, R461.

45 R. D. Priestley, D. Cangialosi and S. Napolitano, *Journal of Non-Crystalline Solids*, 2015, **407**, 288–295.

46 J. H. Mangalara, M. E. Mackura, M. D. Marvin and D. S. Simmons, *Journal of Chemical Physics*, 2017, **146**, 203316.

47 W. Zhang, J. F. Douglas and F. W. Starr, *Proceedings of the National Academy of Sciences*, 2018, **115**, 5641–5646.